Table of Contents

General Method

All reagents and solvents were commercially available and used without further purification, unless otherwise noted. ^{1}H, and ^{13}C NMR spectra were recorded on Bruker Avance III 400 MHz. Mass spectra were determined on Bruker Daltonics Inc. APEXIII 7.0 TESLA FTMS and Agilent 6520 q-TOF LC-MS. The geometry optimization and energy calculation were performed by using Gaussian09 program with B3LYP-D3/6-31G+(d,p) level. Association constants (K_a) were examined by fluorescence titrations on Agilent CaryEclipse Fluorescence Spectrophotometer, where nonlinear curvefitting method was used to obtain the K_a values through the following equation:

$\Delta F = 0.5*(\alpha([G]_0 + [H]_0 + 1/K) - (\alpha\text{^}2([G]_0 + [H]_0 + 1/K)\text{^}2 - 4\alpha^2[H]_0[G]_0)\text{^}0.5)$

Synthesis

The monomer (2,7-bis(2,4-dimethoxy-phenyl) naphthalene) and macrocycle **NBP-OMe** were prepared according to literature procedures (*Angew. Chem. Int. Ed.*, 2020, **59**, 7214–7218.).

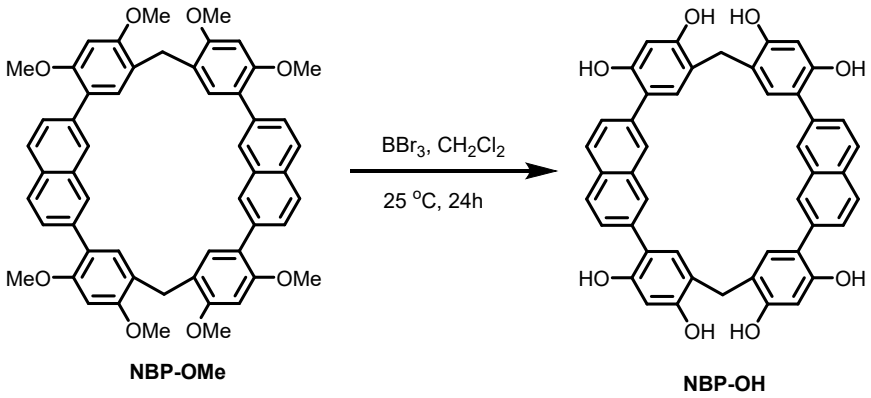

NBP-OMe **NBP-OH**

NBP-OH. To the solution of **NBP-OMe** (1.0 g, 1.2 mmol) in DCM (250 mL) was gradually added BBr_3 (4.1 mL, 46 mmol) and stirred at 25 °C for 24 hours. After pouring the reaction solution into iced water, precipitate appeared and then was filtrated. The per-hydroxylated product **NBP-OH** was obtained (0.24 g, 90%) as brown solid. ^{1}H NMR (400 MHz, CD_3OD) δ (ppm): 7.85 (s, 4H), 7.76 (s, 8H), 7.20 (s, 4H), 6.48 (s, 4H), 3.85 (s, 4H); ^{13}C NMR (100 MHz, DMSO-d_6) δ: 155.3, 153.2, 137.9, 134.1, 132.1, 130.0, 128.3, 126.7, 126.1, 119.2, 118.7, 103.1, 27.7. HRMS (m/z): calcd. for $[M+H]^+$: 713.2170, found 713.2156.

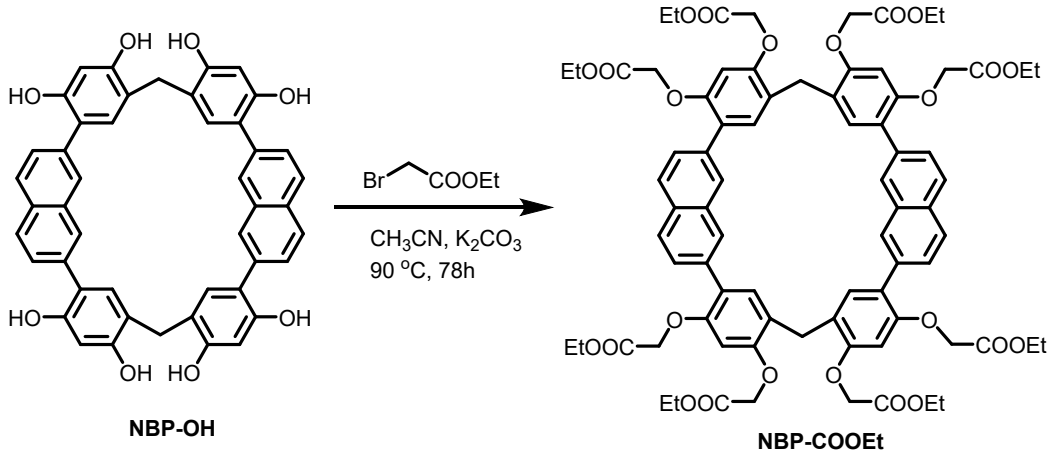

NBP-OH **NBP-COOEt**

NBP-COOEt. To the solution of **NBP-OH** (0.20 g, 0.28 mmol) in MeCN (20 mL) was added K_2CO_3 (0.62 g, 4.5 mmol) and refluxed for 6 hours. Then ethyl bromoacetate (0.37 mL, 3.4 mmol) was added and refluxed for another 72 hours. After filtration, the filtrate was evaporated. The residue was purified by column chromatography (eluent: petroleum ether/ethyl acetate, 1/3, v/v) to afford **NBP-COOEt** as white solid (0.19 g, 48%). ^{1}H NMR (400 MHz, $CDCl_3$) δ (ppm): 7.80 (s, 8H), 7.74 (s, 4H), 7.09 (s, 4H), 6.45 (s, 4H), 4.62 (s, 8H), 4.44 (s, 8H), 4.25 (t, J = 7.2 Hz, 8H), 4.16 (t, J = 7.2 Hz, 8H), 4.11 (s, 4H), 1.25 (t, J = 7.2 Hz, 12H), 1.20 (t, J = 7.2 Hz, 12H); ^{13}C NMR (100 MHz, $CDCl_3$) δ: 169.1, 156.3, 154.4, 136.6, 134.0, 132.9, 131.4, 128.6, 127.7, 126.7, 126.4, 125.3, 123.7, 100.1, 67.0, 66.0, 61.4, 61.3, 28.1, 14.2, 14.2. HRMS (m/z): calcd. for $[M+H]^+$: 1401.5112, found 1401.5119.

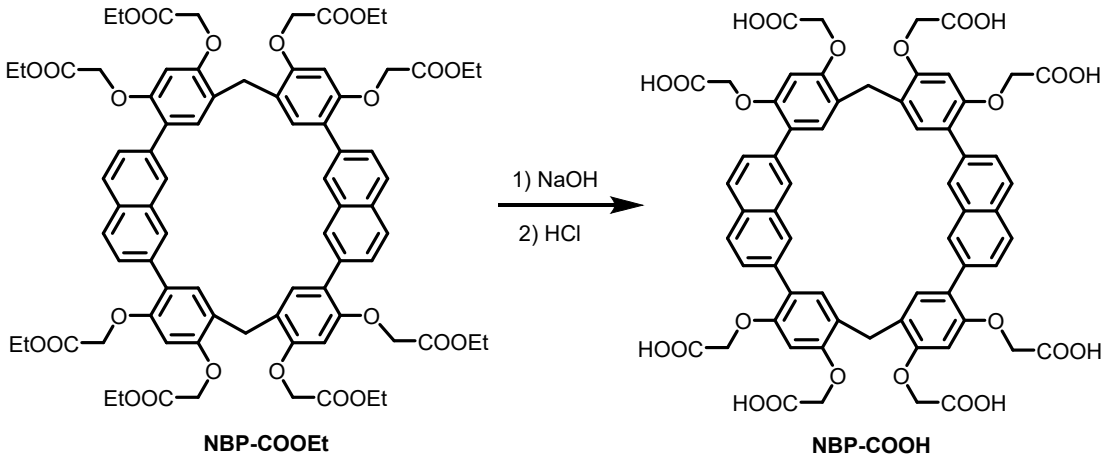

NBP-COOEt **NBP-COOH**

NBP-COOH. To the solution of **NBP-COOEt** (80 mg, 0.057 mmol) in EtOH (4.0 mL) was added NaOH aqueous solution (1.25 ml, 30%) and refluxed for 12 hours. After evaporating the solvent and adding H_2O (8 mL), HCl was added to acidify the solution and adjust the pH to 2-3. The residue was obtained by filtration to afford **NBP-COOH** as dark brown solid (31 mg, 47%). ^{1}H NMR (400 MHz, DMSO-d_6) δ (ppm): 7.88 (s, 4H), 7.80 (m, 8H), 6.96 (s, 4H), 6.65 (s, 4H), 4.72 (s, 8H), 4.65 (s, 8H), 3.97 (s, 4H); ^{13}C NMR (100 MHz, DMSO-d_6) δ: 170.3, 156.1, 153.9, 137.0, 133.8, 132.1, 130.6, 128.6, 126.9, 126.2, 122.8, 121.3, 98.3, 65.4, 65.2, 40.0, 27.6. HRMS (m/z): calcd. for $[M+Na]^+$: 1199.2433, found 1199.2428; calcd. for $[M+NH_4]^+$: 1194.2879, found 1194.281.

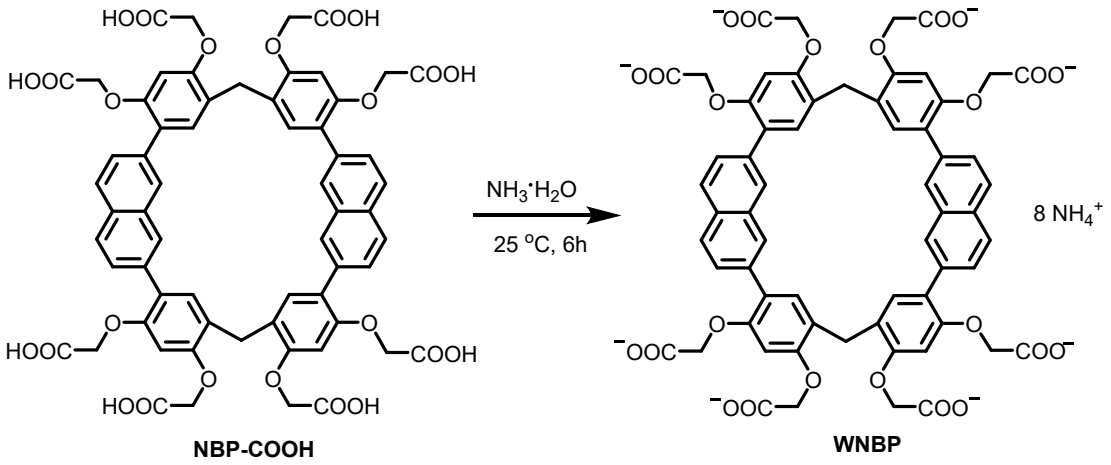

WNBP. The solution of **NBP-COOH** (0.2 g, 0.17 mmol) in $NH_3 \cdot H_2O$ (60 mL) was stirred at 25 °C for 6 hours. After evaporating the solvent, the water-soluble macrocycle **WNBP** was obtained as brown solid (0.18 g, 81%). ^{1}H NMR (400 MHz, D_2O) δ (ppm): 7.98 (s, 4H), 7.94 (d, J = 8.4 Hz, 4H), 7.86 (d, J = 8.0 Hz, 4H), 7.19 (s, 4H), 6.47 (s, 4H), 4.48 (s, 8H), 4.40 (s, 8H), 4.10 (s, 4H); ^{13}C NMR (100 MHz, D_2O) δ: 201.7, 189.4, 182.1, 177.0, 171.8, 161.0, 158.2, 154.8, 151.7, 136.3, 134.1, 132.6, 131.4, 128.7, 127.3, 127.1, 122.5, 121.2, 99.8, 70.5, 68.1, 67.2, 65.5, 26.2. HRMS (m/z): calcd. for $[M\text{-}8NH_4]^{8-}$: 146.02387, found 146.02362.

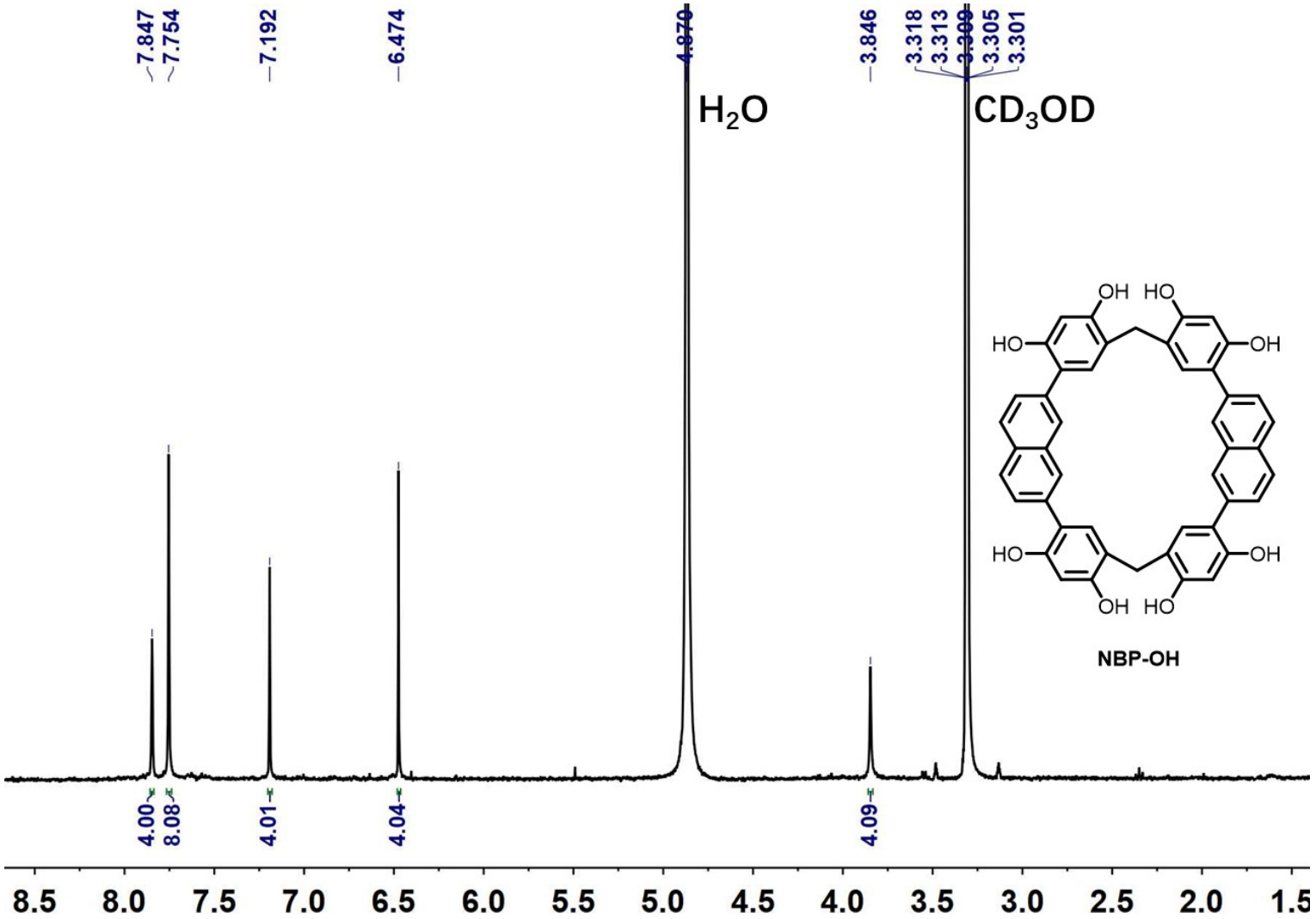

Figure S1. ^{1}H NMR spectrum (400 MHz, CD_3OD, 298K) of **NBP-OH**.

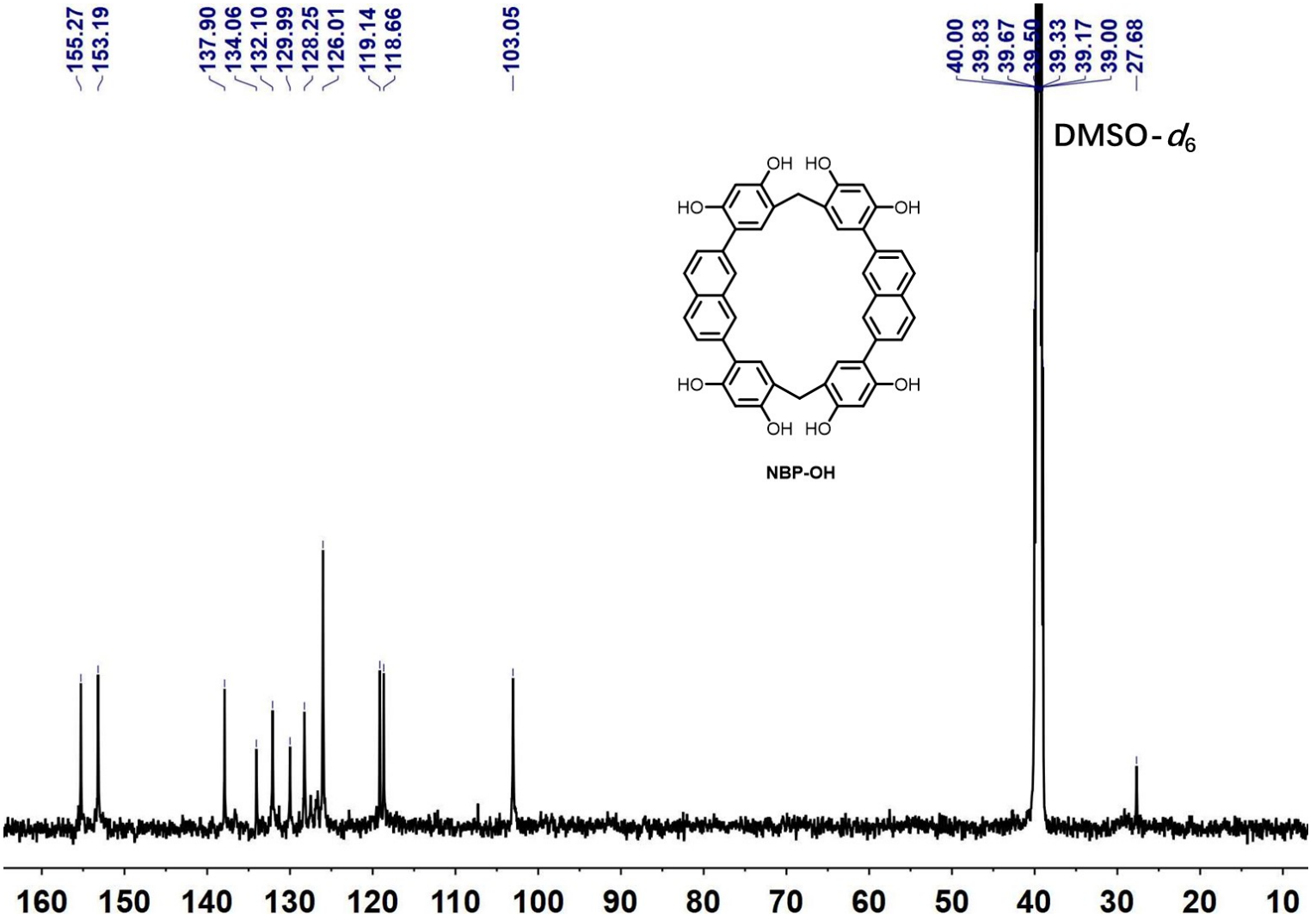

Figure S2. ^{13}C NMR spectrum (100 MHz, DMSO-d_6, 298K) of **NBP-OH**.

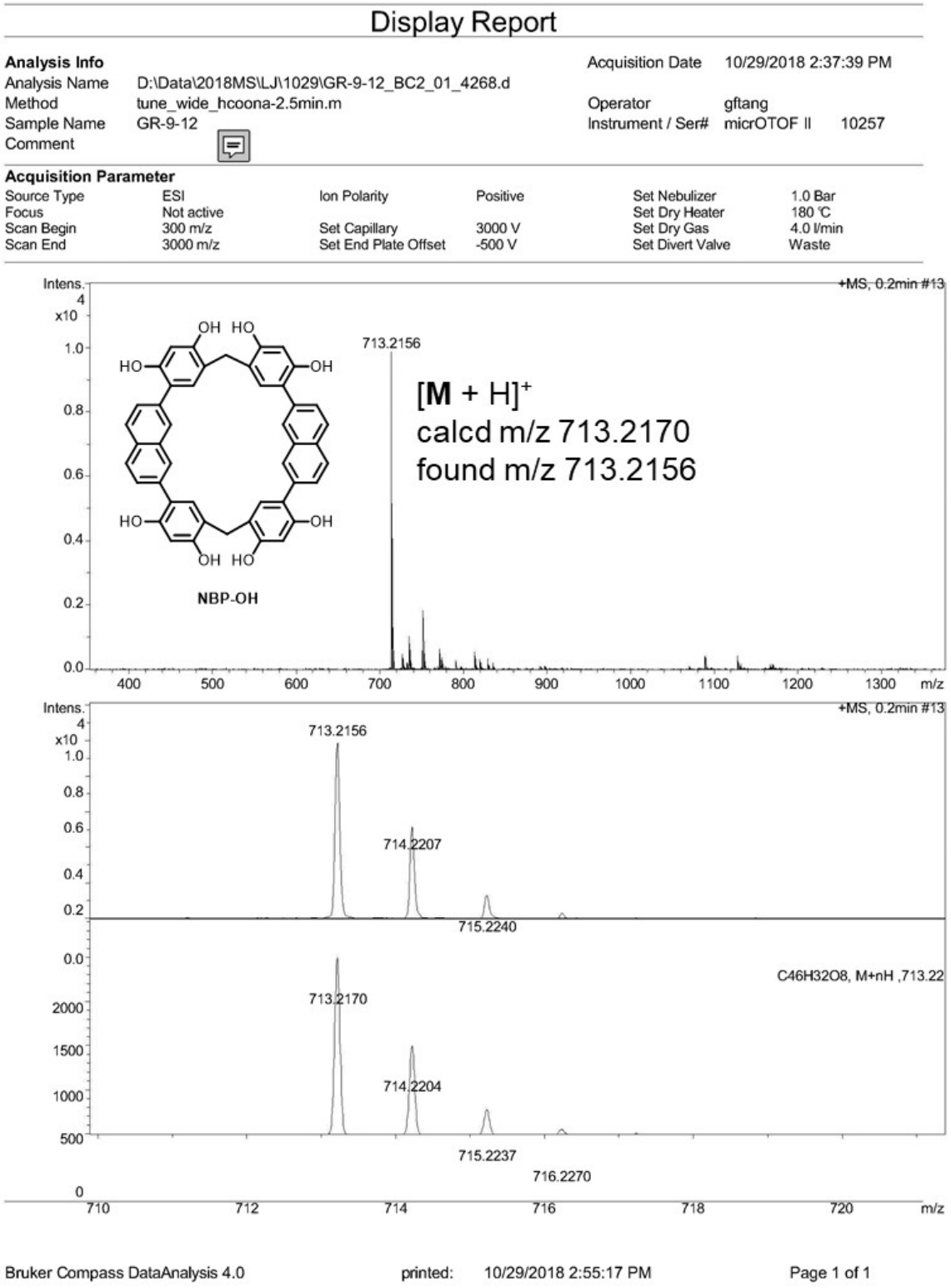

Figure S3. HRMS spectrum of **NBP-OH**.

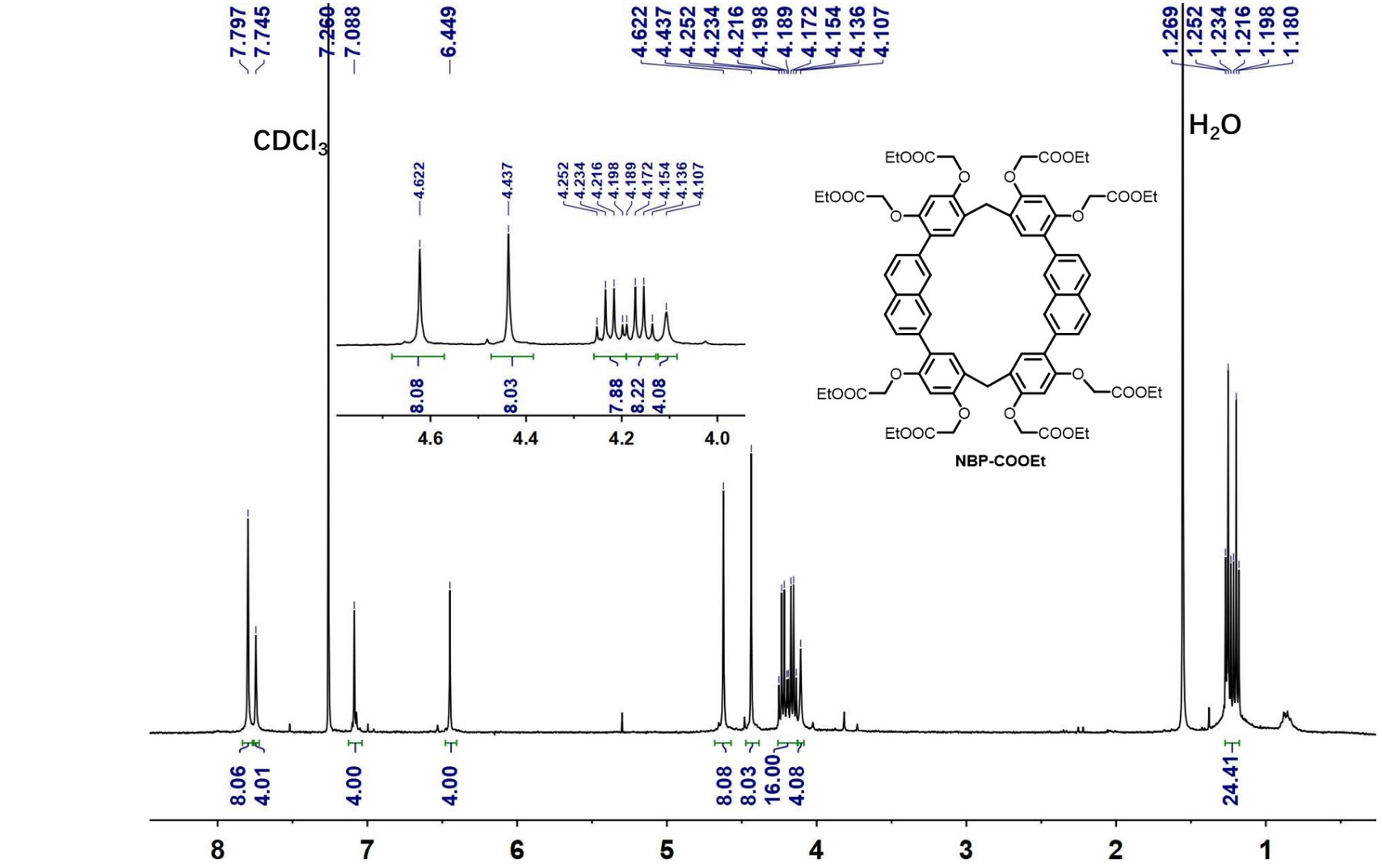

Figure S4. ^{1}H NMR spectrum (400 MHz, $CDCl_3$, 298K) of **NBP-COOEt**.

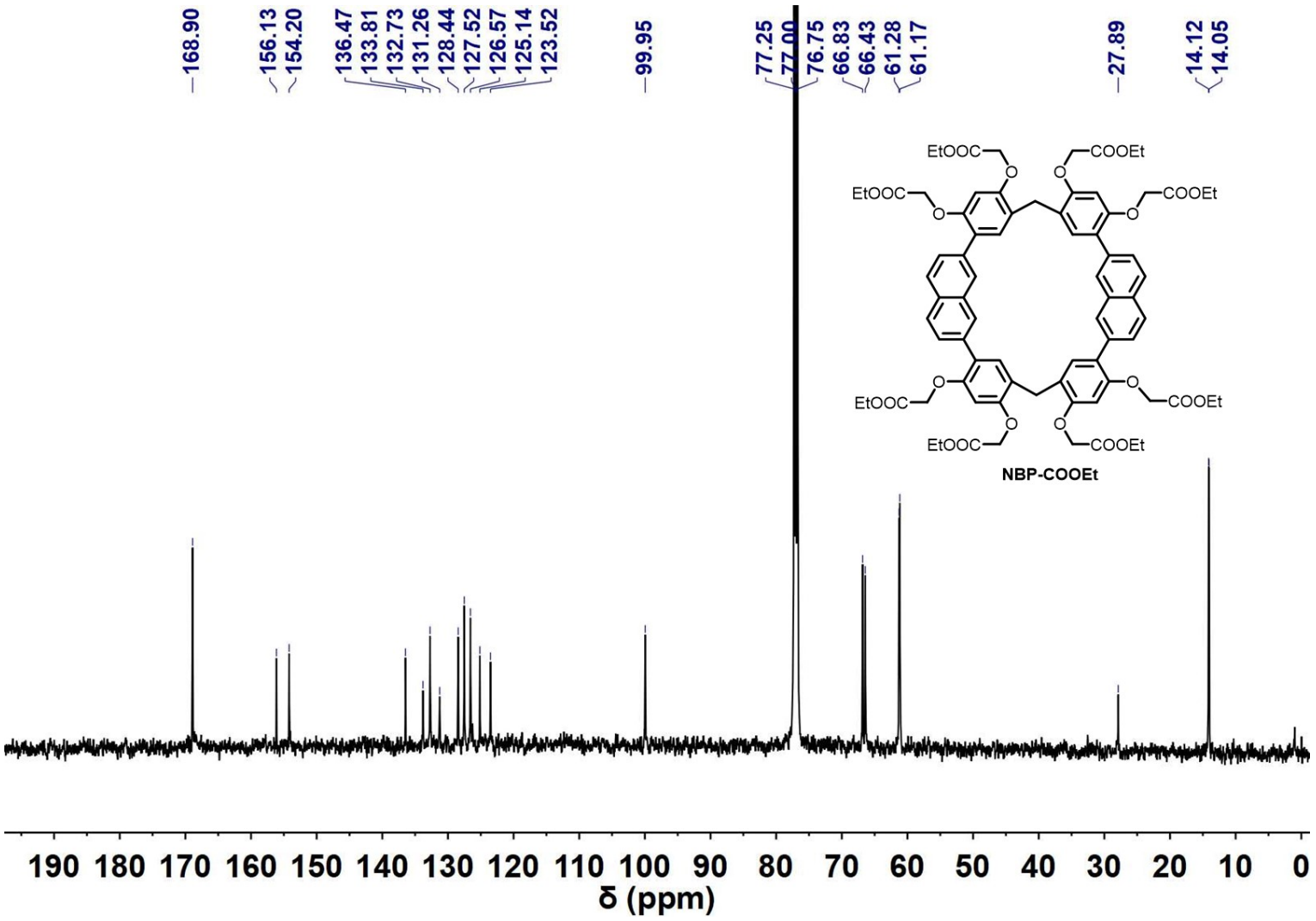

Figure S5. ^{13}C NMR spectrum (100 MHz, $CDCl_3$, 298K) of **NBP-COOEt**.

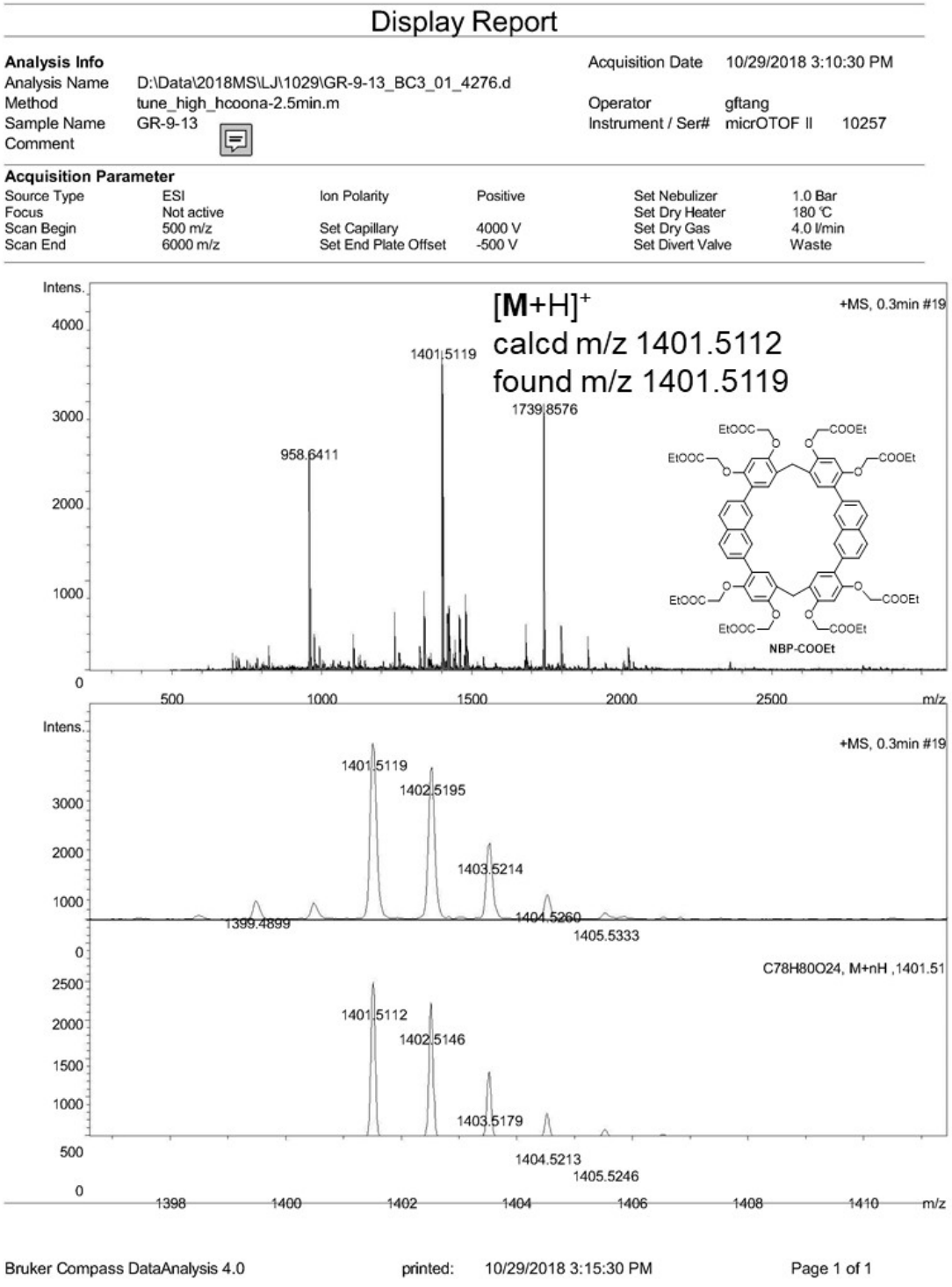

Figure S6. HRMS spectrum of **NBP-COOEt**.

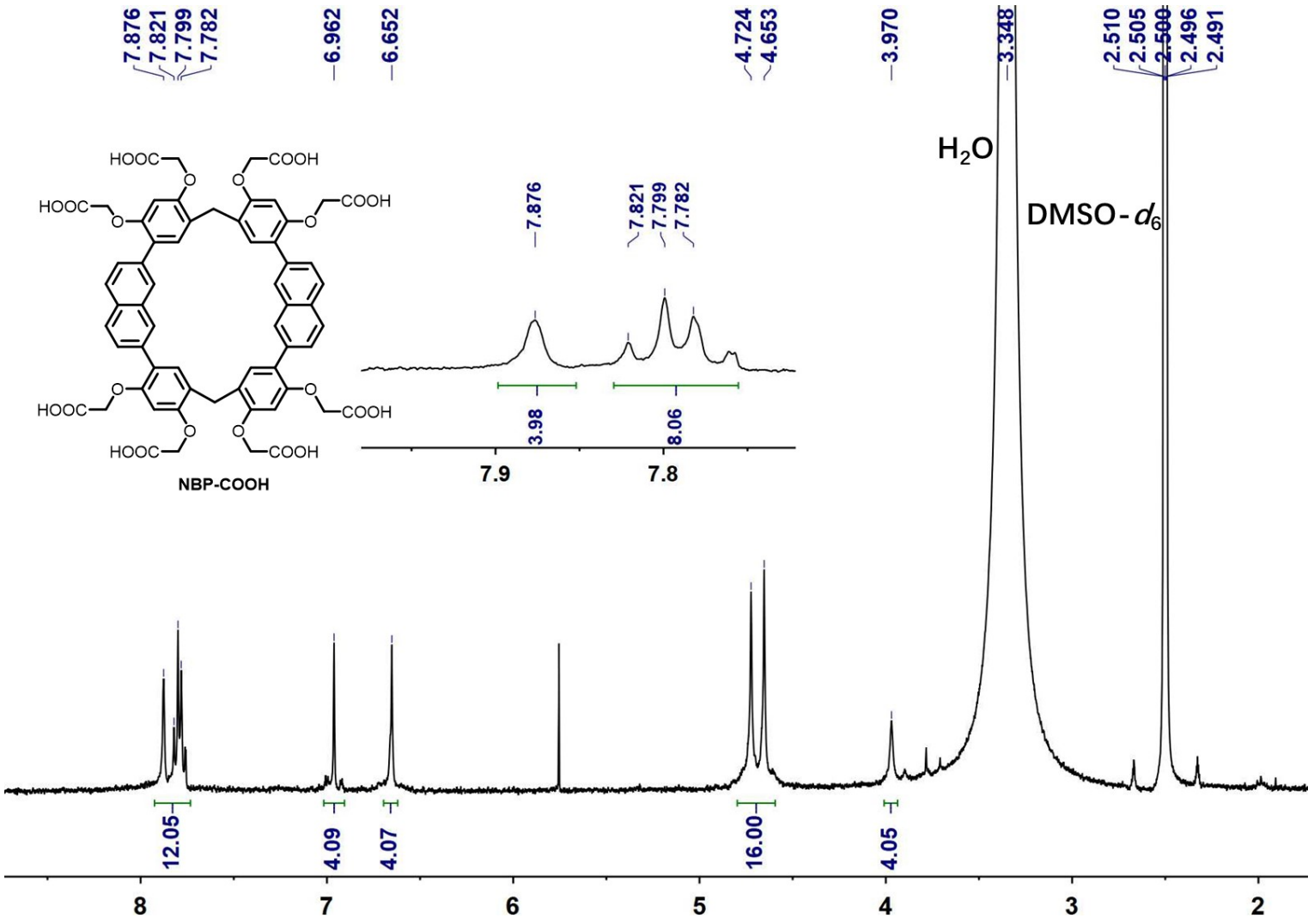

Figure S7. ^{1}H NMR spectrum (400 MHz, DMSO-d_6, 298K) of **NBP-COOH**.

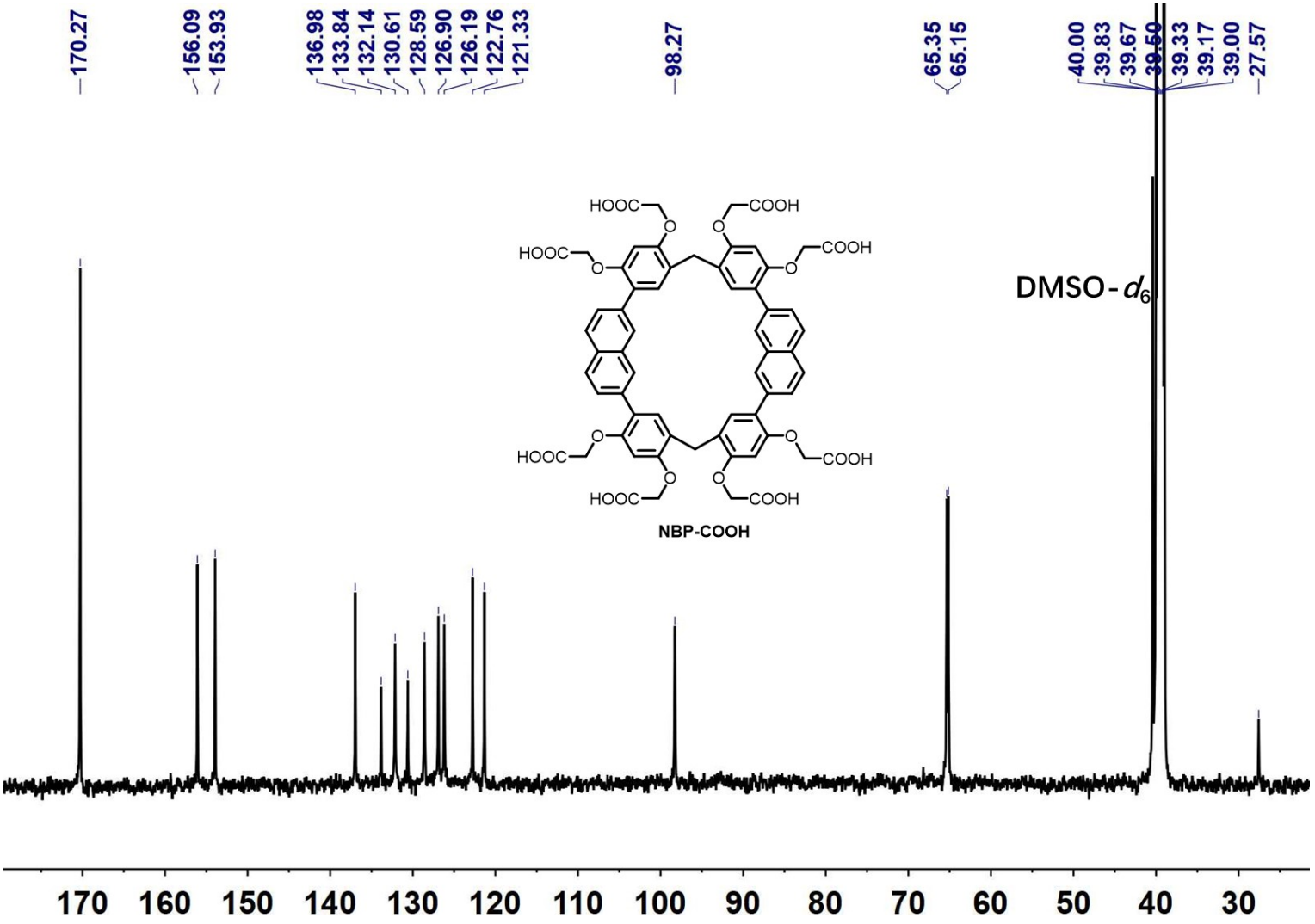

Figure S8. ^{13}C NMR spectrum (100 MHz, DMSO-d_6, 298K) of **NBP-COOH**.

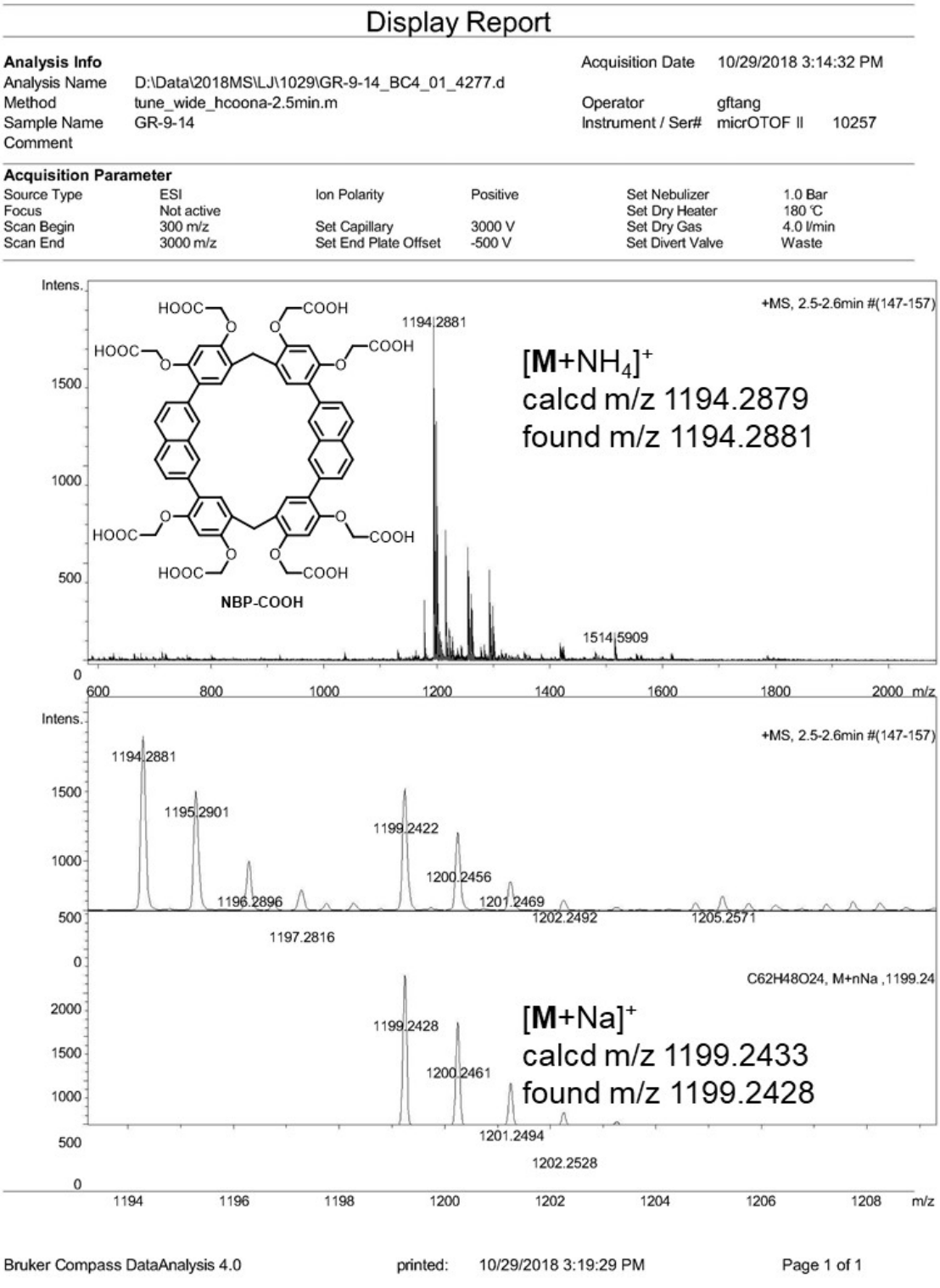

Figure S9. HRMS spectrum of **NBP-COOH**.

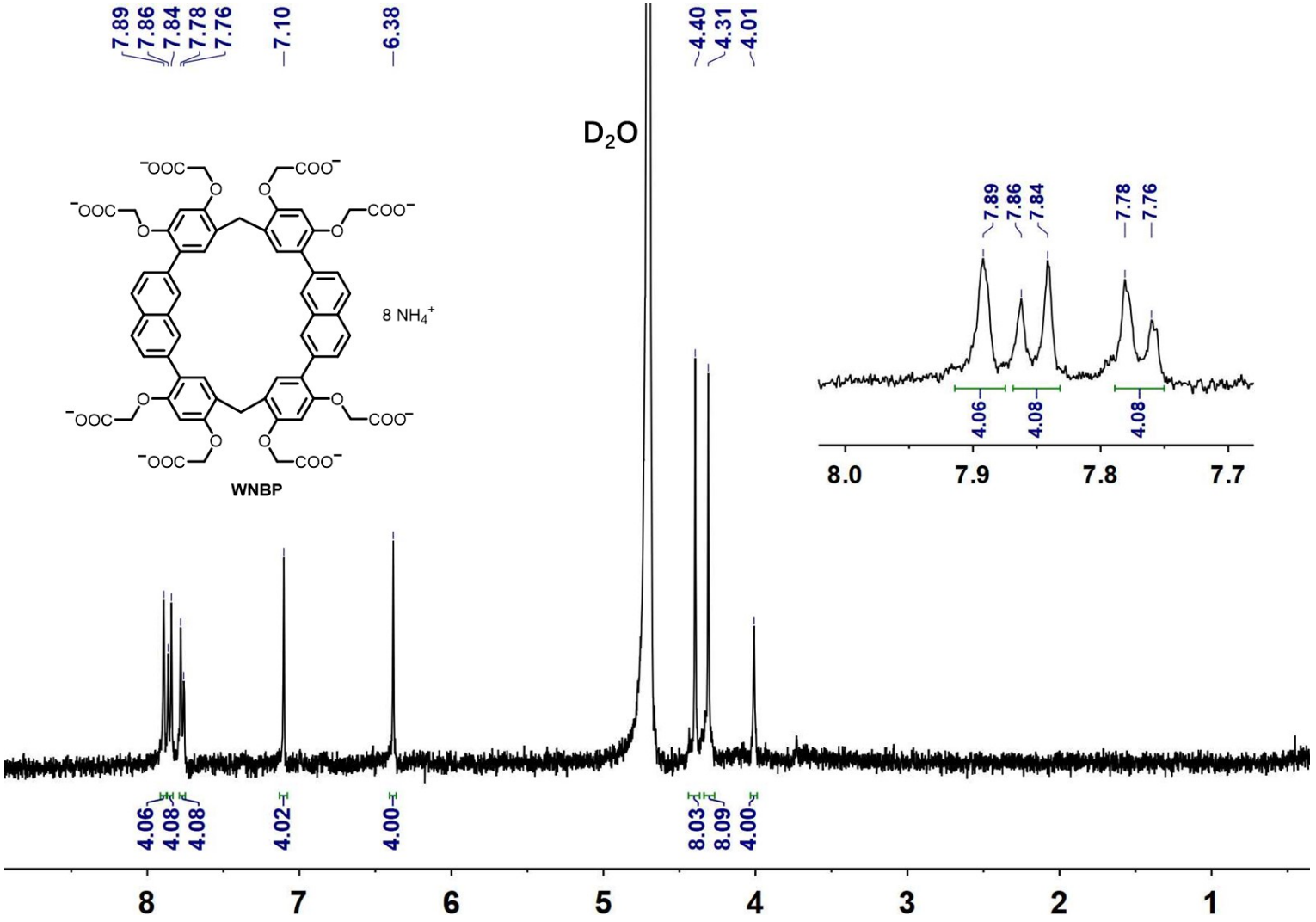

Figure S10. ^{1}H NMR spectrum (400 MHz, D_2O, 298K) of **WNBP**.

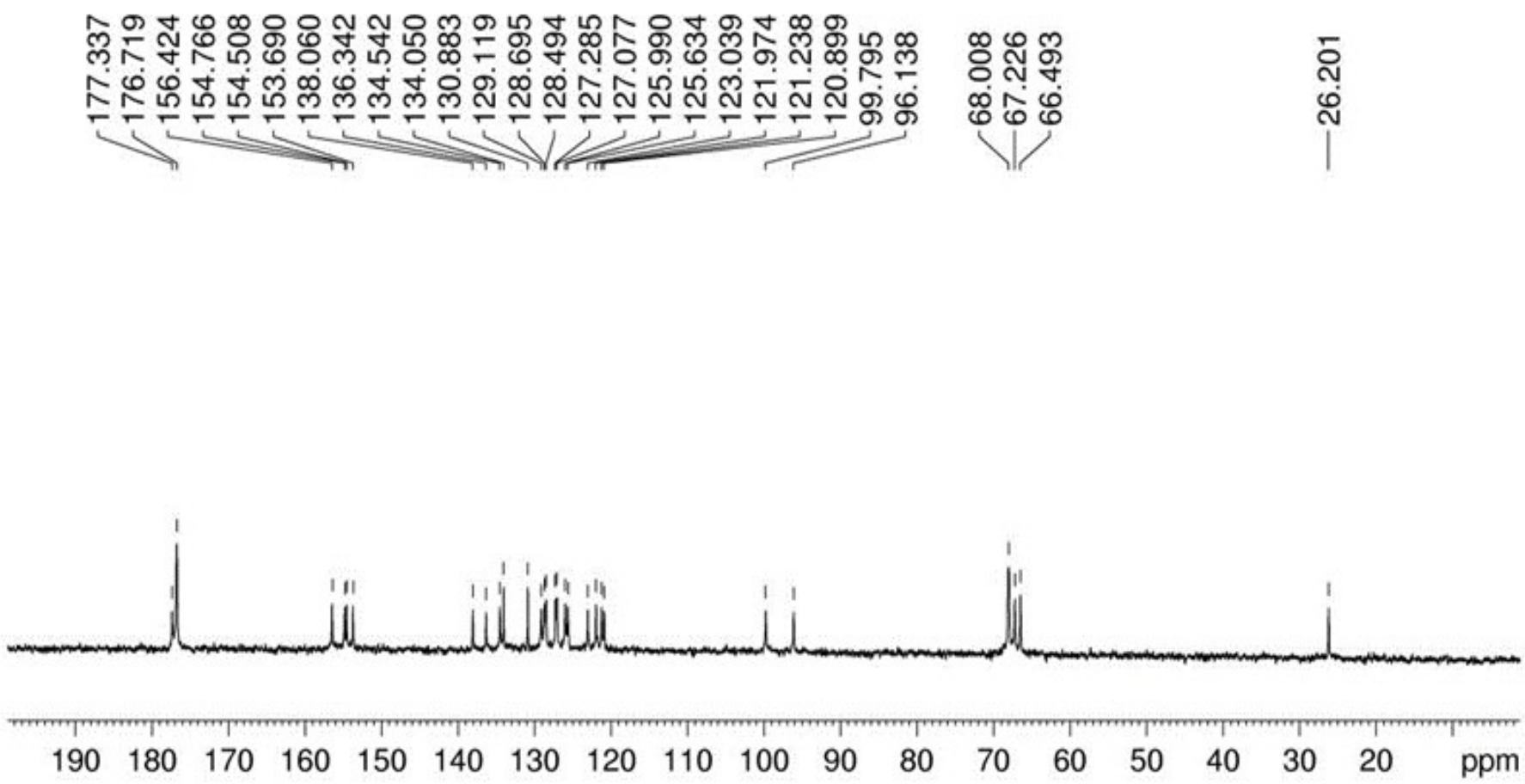

Figure S11. ^{13}C NMR spectrum (100 MHz, D_2O, 298K) of **WNBP**.

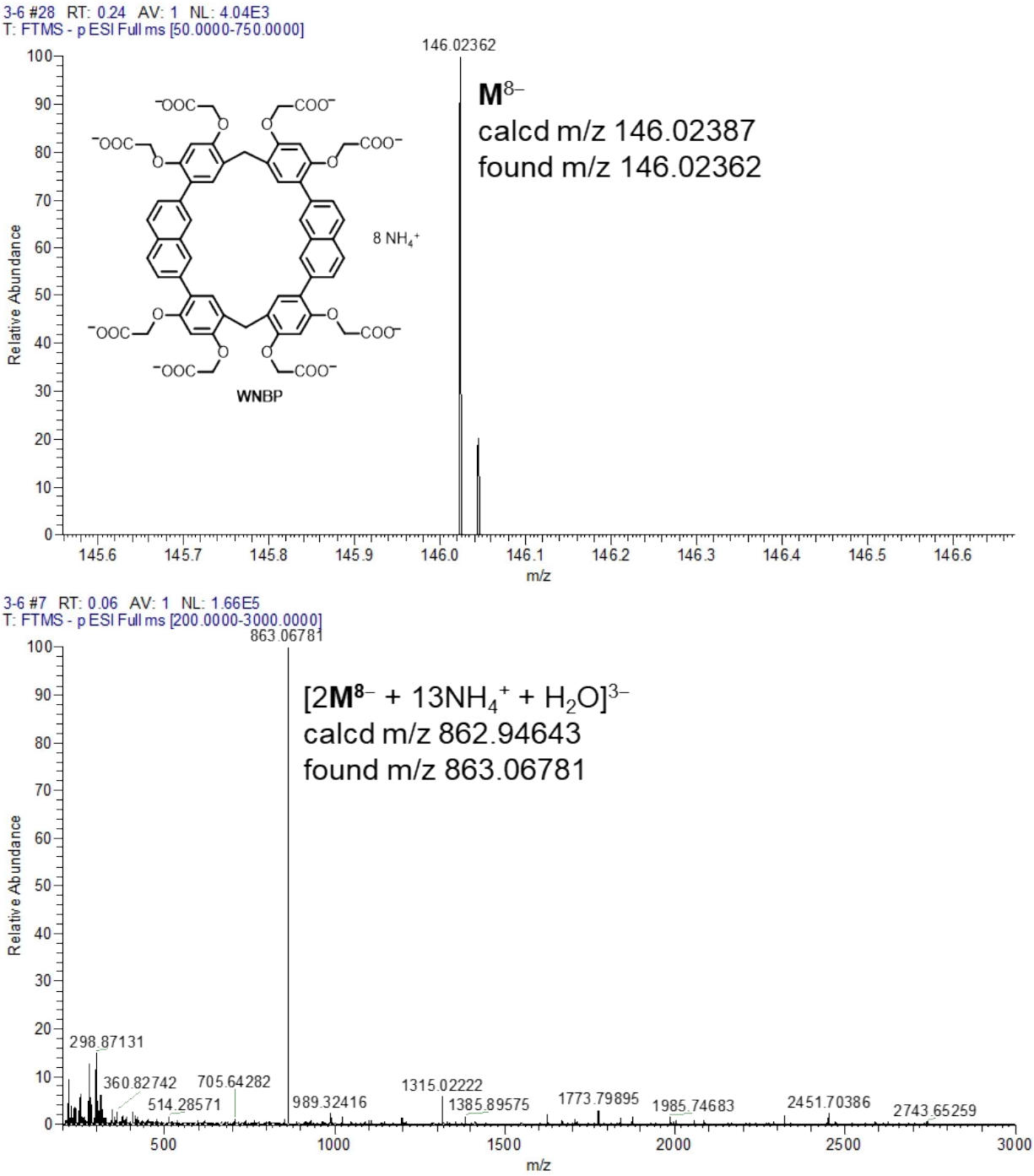

Figure S12. HRMS spectrum of **WNBP**.

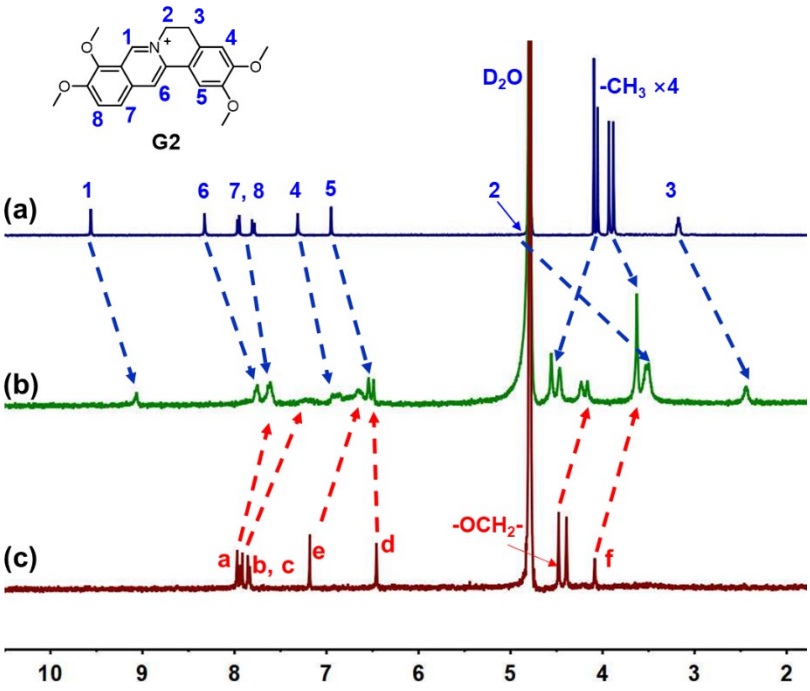

Figure S13. Partial ^{1}H NMR spectra (400 MHz, 0.8 mM, D_2O) of macrocycle **WNBP** in the presence of **G2**. (a) **G2**, (b) **WNBP** + **G2**, (c) **WNBP**.

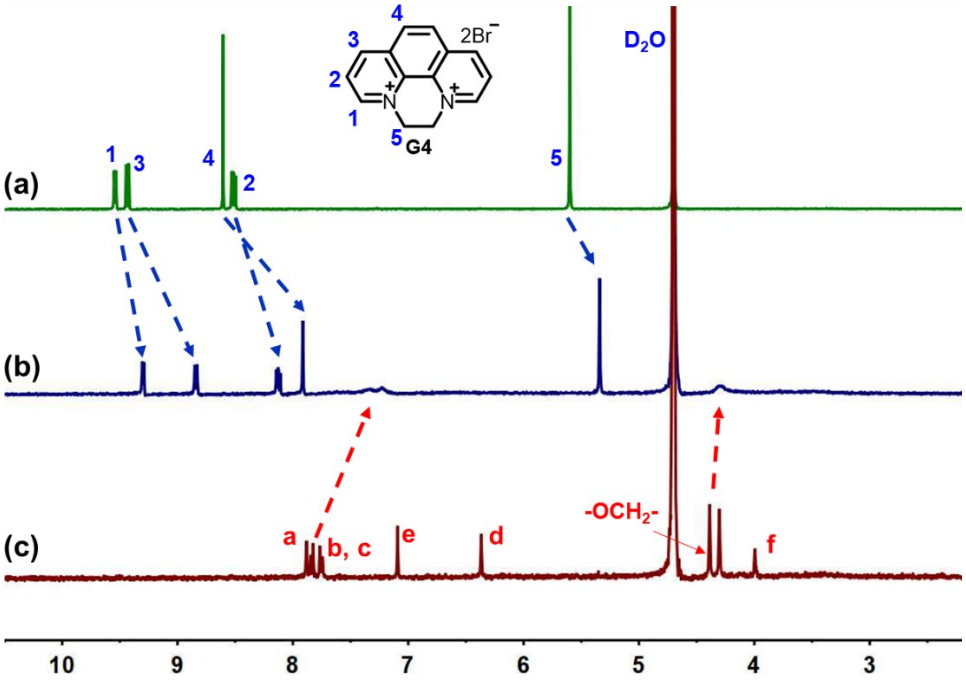

Figure S14. Partial ^{1}H NMR spectra (400 MHz, 0.8 mM, D_2O) of macrocycle **WNBP** in the presence of **G4**. (a) **G4**, (b) **WNBP** + **G4**, (c) **WNBP**.

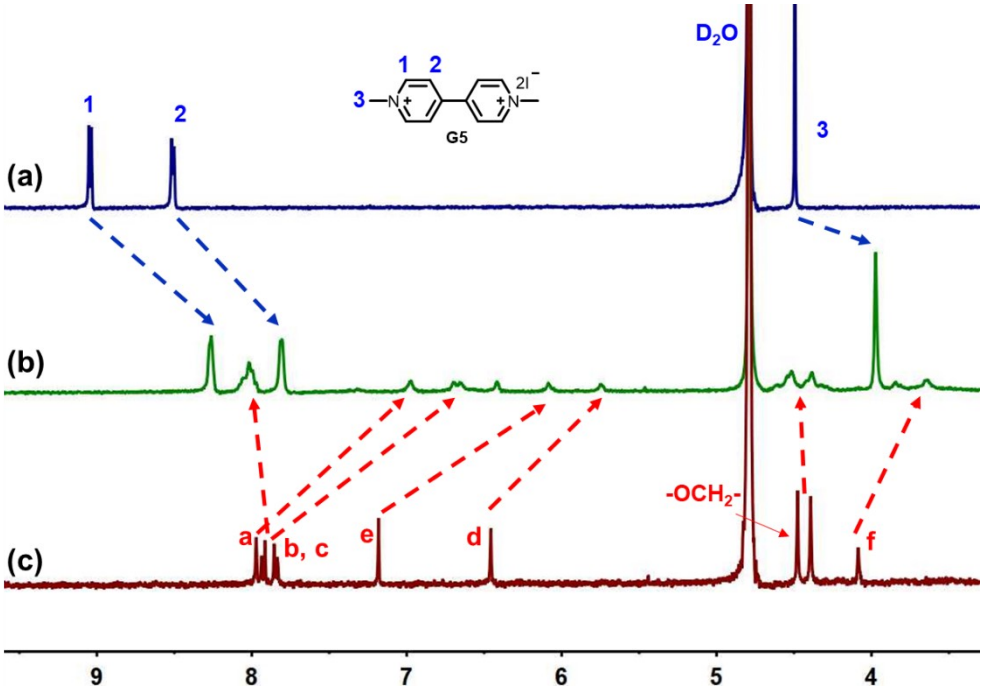

Figure S15. Partial ^{1}H NMR spectra (400 MHz, 0.8 mM, D_2O) of macrocycle **WNBP** in the presence of **G5**. (a) **G5**, (b) **WNBP** + **G5**, (c) **WNBP**.

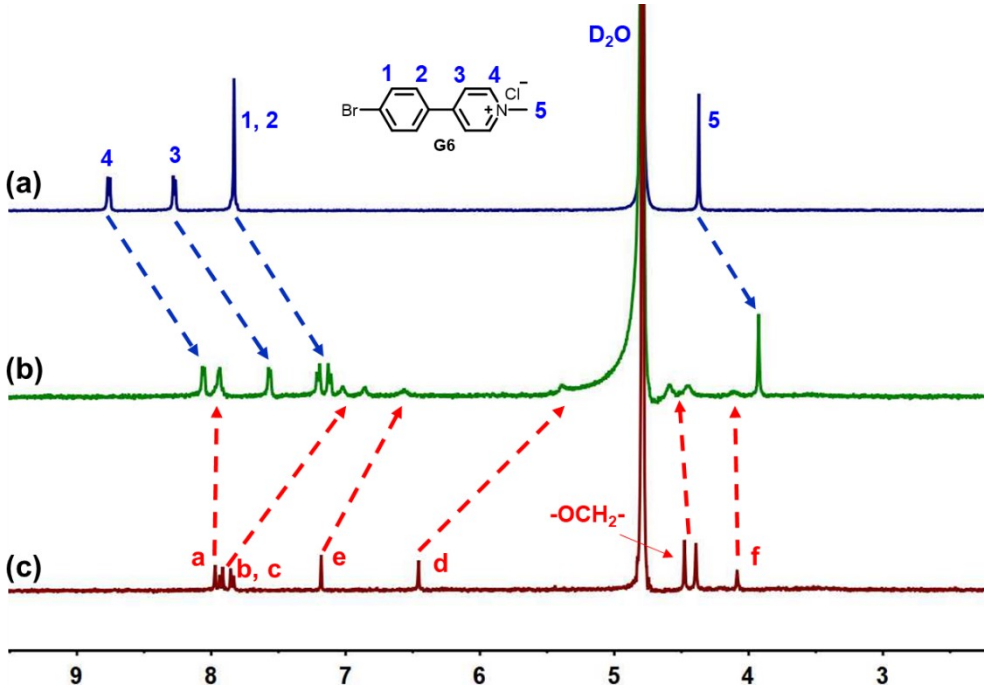

Figure S16. Partial ^{1}H NMR spectra (400 MHz, 0.8 mM, D_2O) of macrocycle **WNBP** in the presence of **G6**. (a) **G6**, (b) **WNBP** + **G6**, (c) **WNBP**.

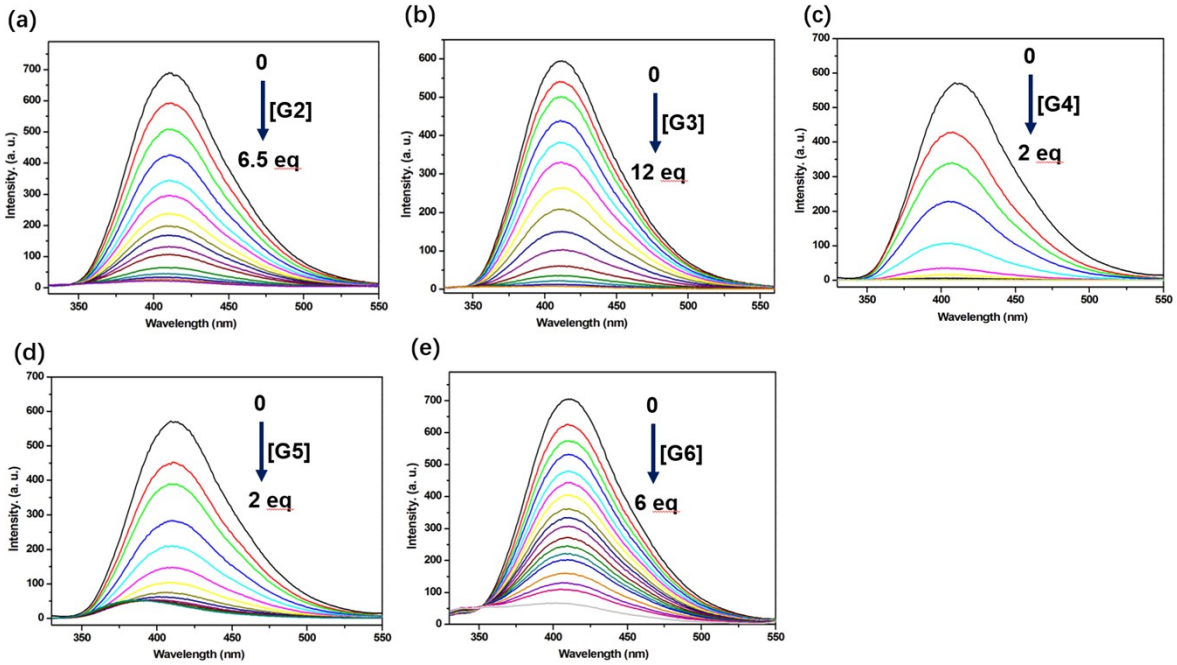

Figure S17. Fluorescence spectra of **WNBP** (1.0 μM) in aqueous solution recorded in the presence of different concentrations of guests at 298 K. (a) **G2**, (b) **G3**, (c) **G4**, (d) **G5**, (e) **G6**.

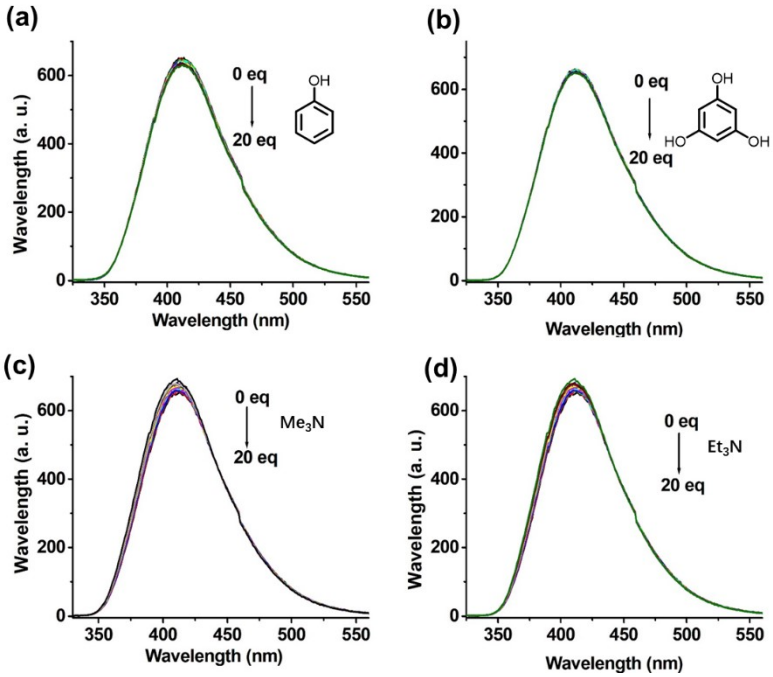

Figure S18. Fluorescence spectra of **WNBP** (1.0 μM) in aqueous solution recorded in the presence of different concentrations of (a) **G7**, (b) **G8**, (c) **G9** and (d) G**10**.

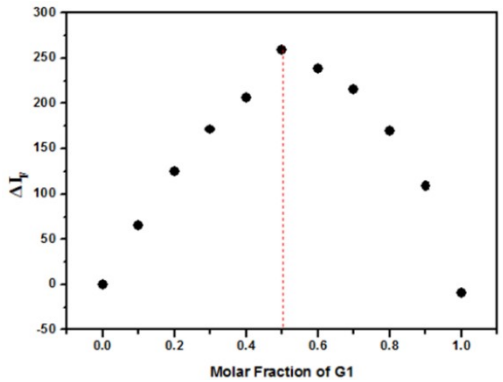

Figure S19. Job's plot obtained by plotting the fluorescence intensity change (ΔF) of **WNBP** by varying the ratio of the host and guests against the mole fraction of guest. The total concentration of the host and the guest is fixed: [Host] + [Guest] = 2.0 mM.

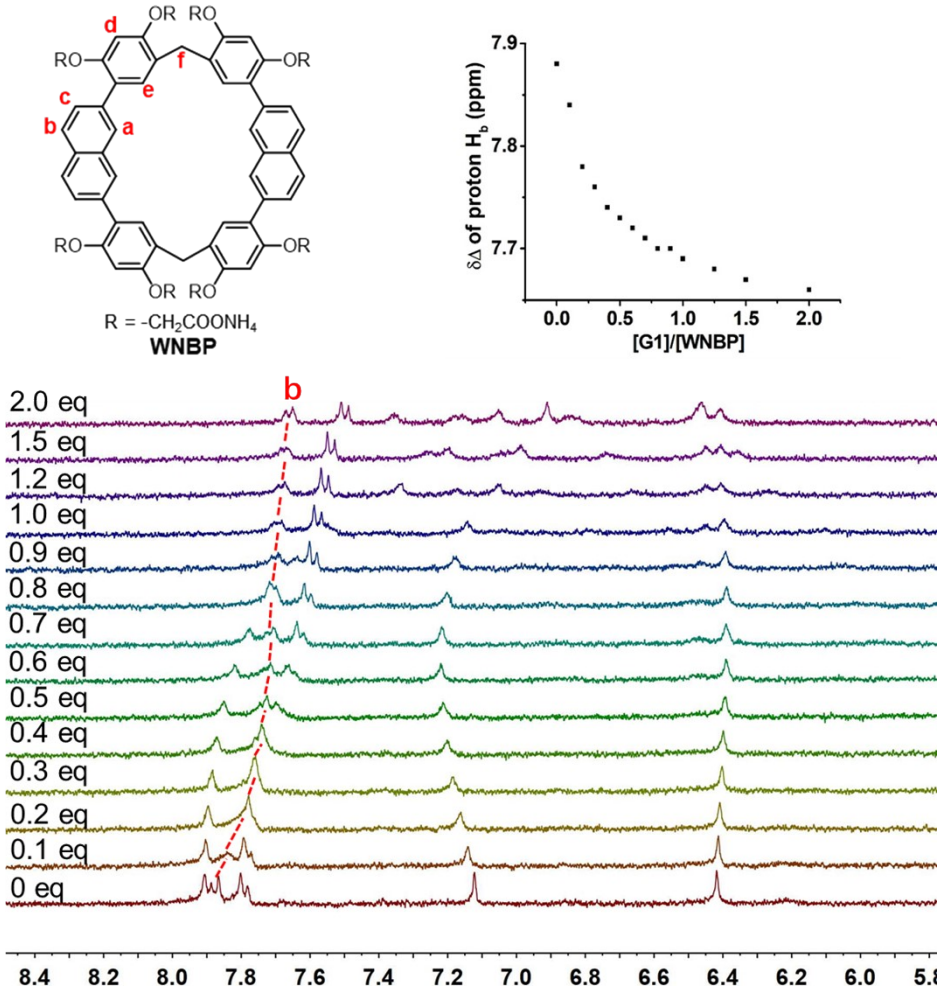

Figure S20. Partial ^{1}H NMR spectra (400 MHz, 0.8 mM, D_2O) of **WNBP** in the presence of different concentrations of **G1**.

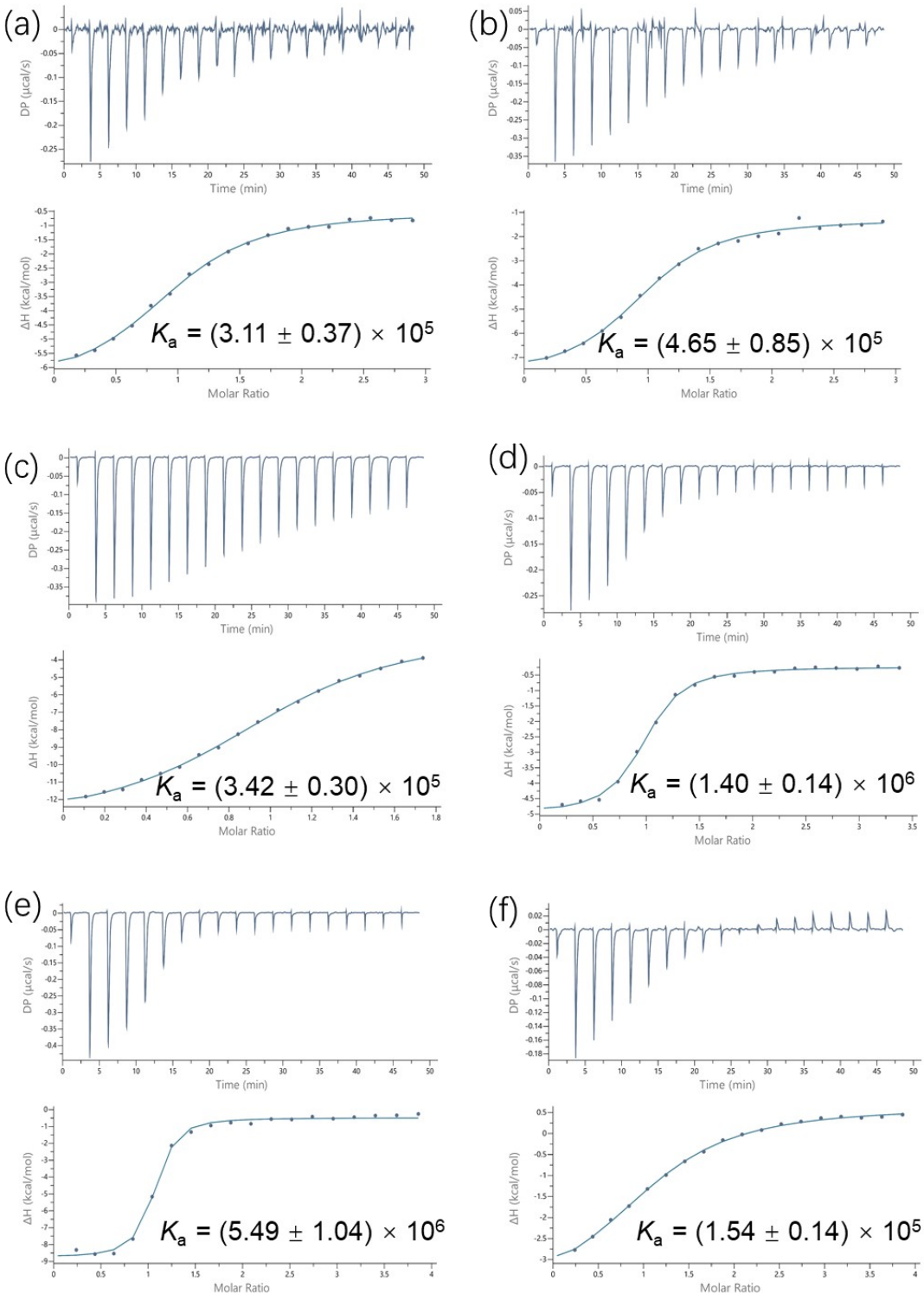

Figure S21. Titration plots (heat flow versus time and heat flow versus molar ratio) obtained from ITC experiments of **WNPB** with (a) **G1**, (b)**G2**, (c)**G3**, (d)**G4**, (e)**G5** and (f) **G6** in phosphate buffer (10 mM, pH=7.00).

Table S1. Association constants (K_a, M^{-1}) of **WNBP** with the cationic guests in different solution mediums at 298 K.

	K_a (in H_2O)	K_a (in phosphate buffer, 10 mM, [illegible])	K_a (in phosphate buffer, 10 mM, [illegible])	K_a (in phosphate buffer, 10 mM, [illegible])
G1	$(7.08 \pm 0.80) \times 10^6$	$(3.73 \pm 0.42) \times 10^6$	$(1.51 \pm 0.19) \times 10^6$	$(1.03 \pm 0.32) \times 10^7$
G2	$(1.06 \pm 0.16) \times 10^6$	$(4.28 \pm 1.09) \times 10^6$	$(1.80 \pm 0.38) \times 10^6$	$(2.43 \pm 0.22) \times 10^6$
G3	$(2.29 \pm 0.27) \times 10^6$	$(2.91 \pm 0.59) \times 10^6$	$(1.67 \pm 0.45) \times 10^6$	$(2.77 \pm 0.53) \times 10^6$
G4	$(1.30 \pm 0.28) \times 10^7$	$(8.74 \pm 2.09) \times 10^7$	$(2.66 \pm 0.69) \times 10^7$	$(7.53 \pm 1.65) \times 10^6$
G5	$(1.26 \pm 0.40) \times 10^6$	$(7.83 \pm 2.82) \times 10^6$	$(2.24 \pm 0.64) \times 10^6$	$(3.17 \pm 1.08) \times 10^6$
G6	$(3.17 \pm 0.52) \times 10^6$	$(4.12 \pm 0.81) \times 10^6$	$(3.52 \pm 1.27) \times 10^6$	$(1.47 \pm 0.71) \times 10^6$

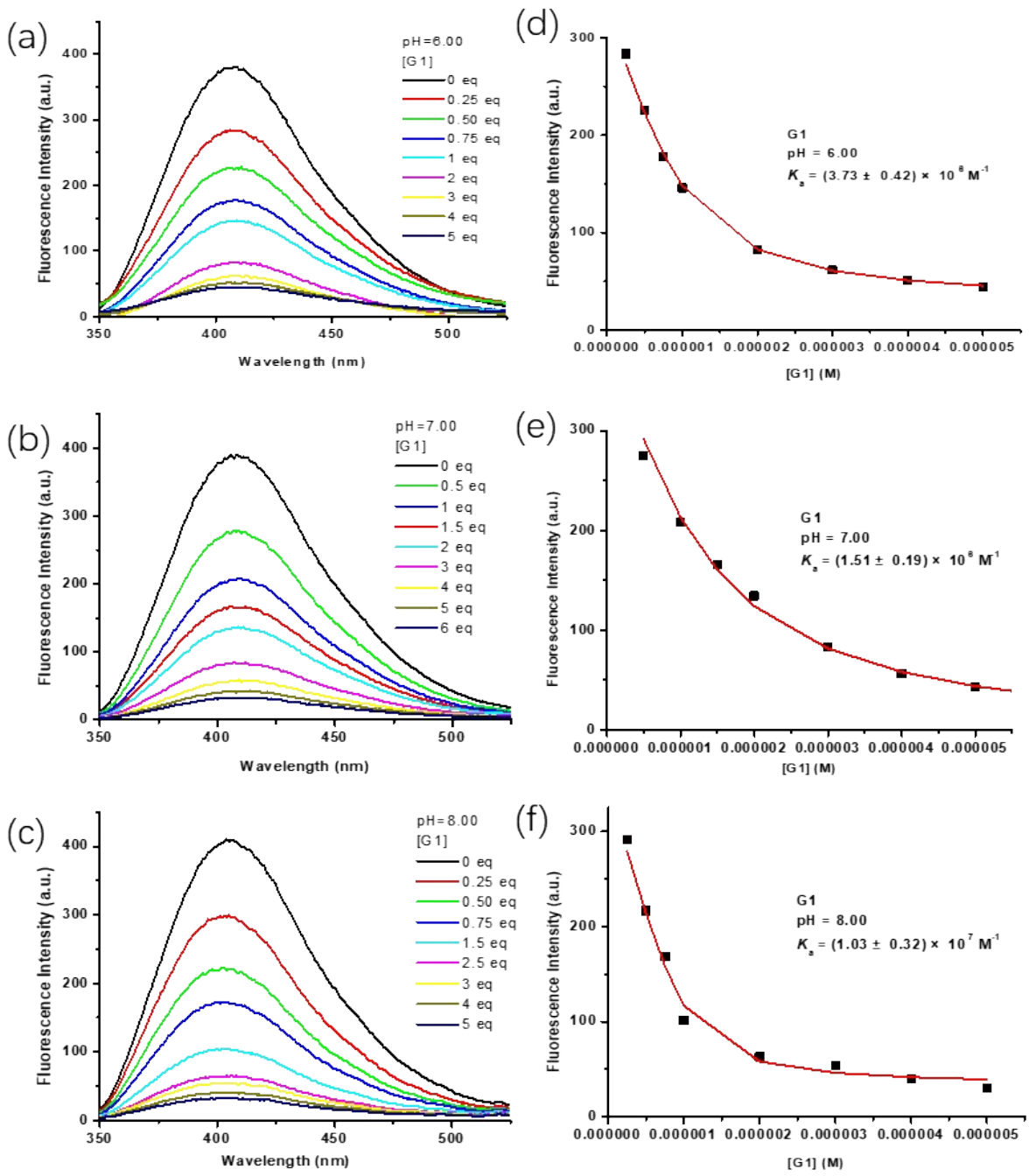

Figure S22. Fluorescence spectra of **WNBP** (1.00 μM) in phosphate buffer solutions (1.0 mM) recorded in the presence of different concentrations of **G1** at 298 K, (a) pH=6.00, (b) pH=7.00, (c) pH=8.00. Nonlinear least-squares analyses used to calculate the K_a value, (d) pH=6.00, (e) pH=7.00, (f) pH=8.00.

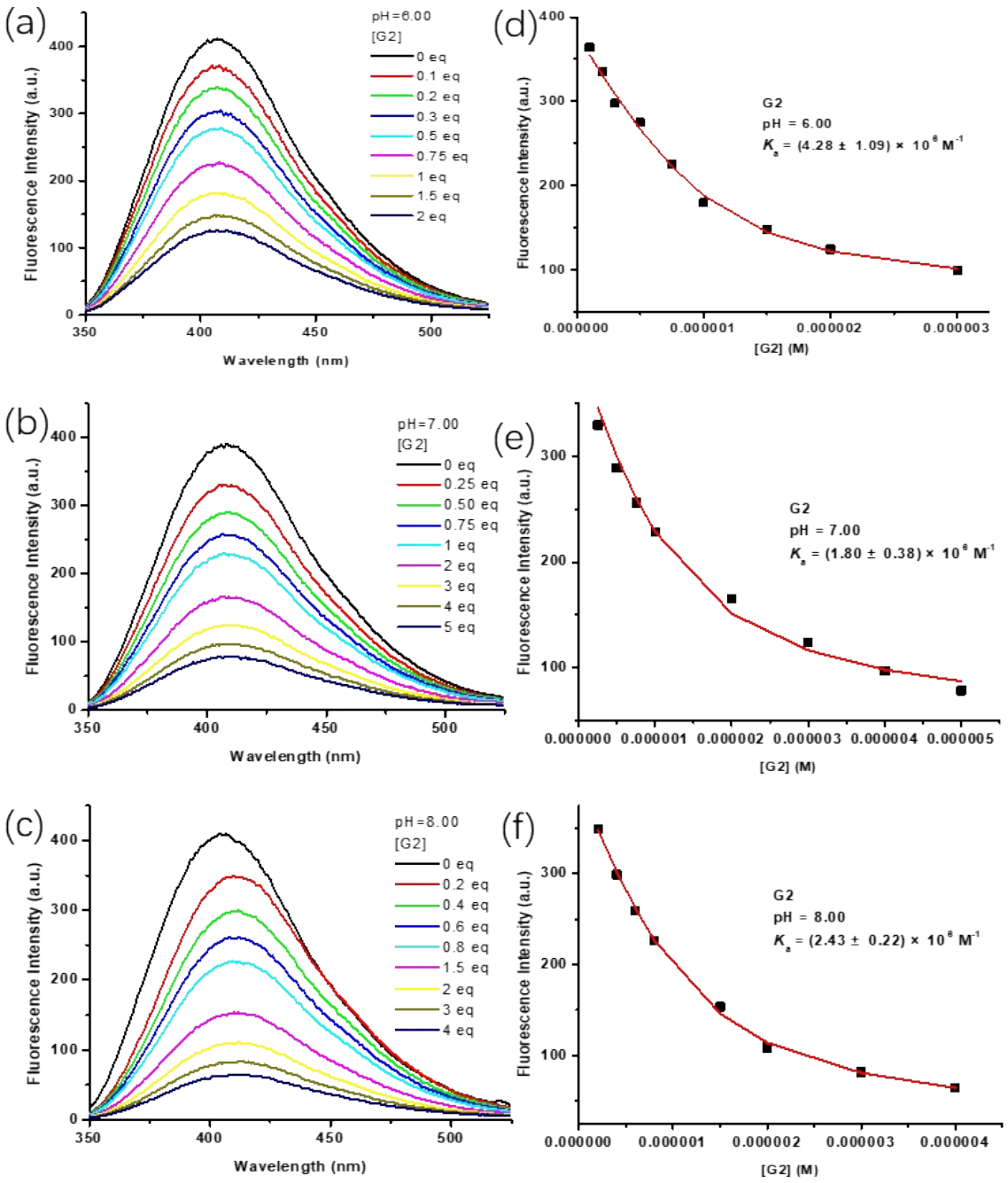

Figure S23. Fluorescence spectra of **WNBP** (1.00 μM) in phosphate buffer solutions (1.0 mM) recorded in the presence of different concentrations of **G2** at 298 K, (a) pH=6.00, (b) pH=7.00, (c) pH=8.00. Nonlinear least-squares analyses used to calculate the K_a value, (d) pH=6.00, (e) pH=7.00, (f) pH=8.00.

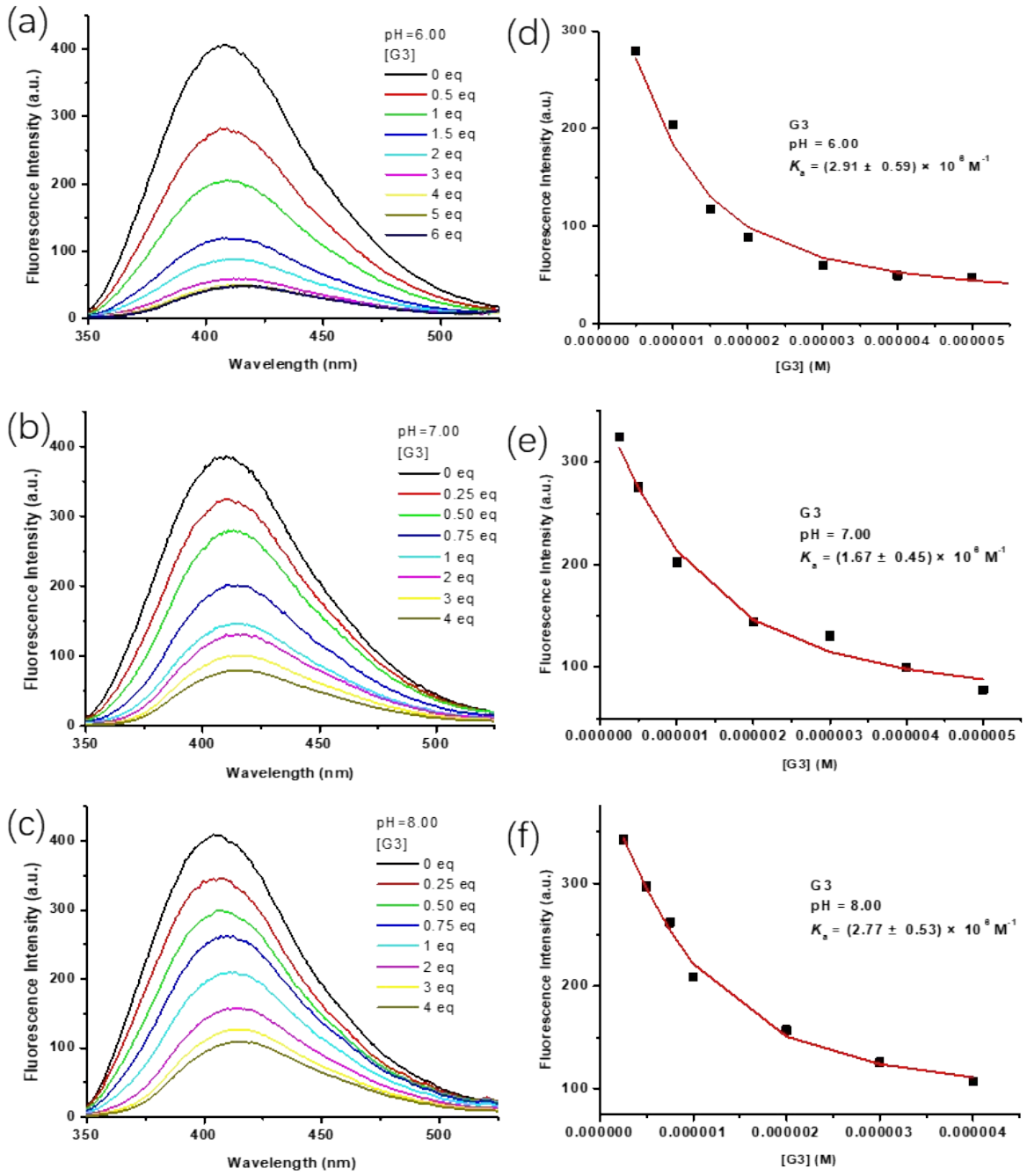

Figure S24. Fluorescence spectra of **WNBP** (1.00 μM) in phosphate buffer solutions (1.0 mM) recorded in the presence of different concentrations of **G3** at 298 K, (a) pH=6.00, (b) pH=7.00, (c) pH=8.00. Nonlinear least-squares analyses used to calculate the K_a value, (d) pH=6.00, (e) pH=7.00, (f) pH=8.00.

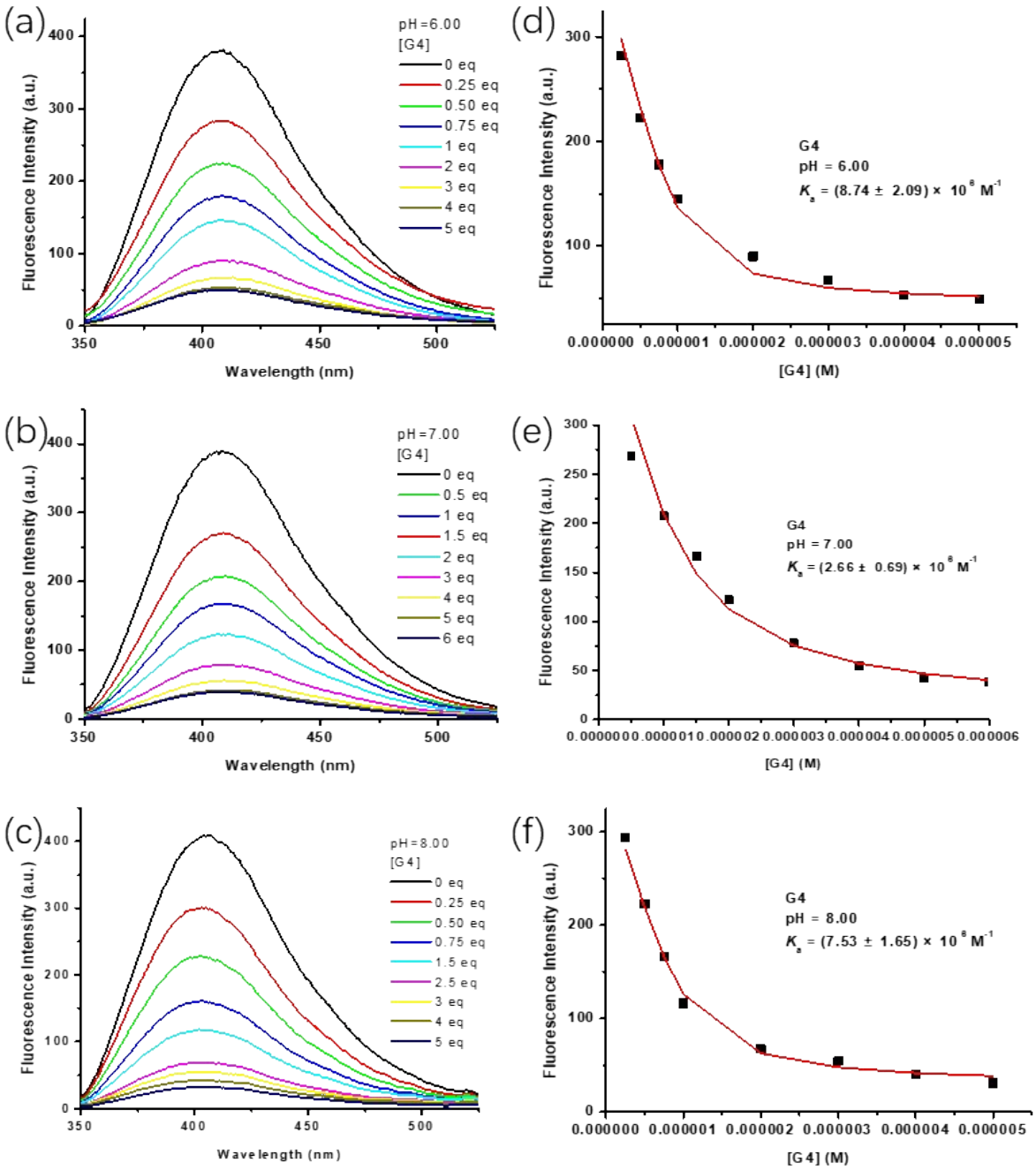

Figure S25. Fluorescence spectra of **WNBP** (1.00 μM) in phosphate buffer solutions (1.0 mM) recorded in the presence of different concentrations of **G4** at 298 K, (a) pH=6.00, (b) pH=7.00, (c) pH=8.00. Nonlinear least-squares analyses used to calculate the K_a value, (d) pH=6.00, (e) pH=7.00, (f) pH=8.00.

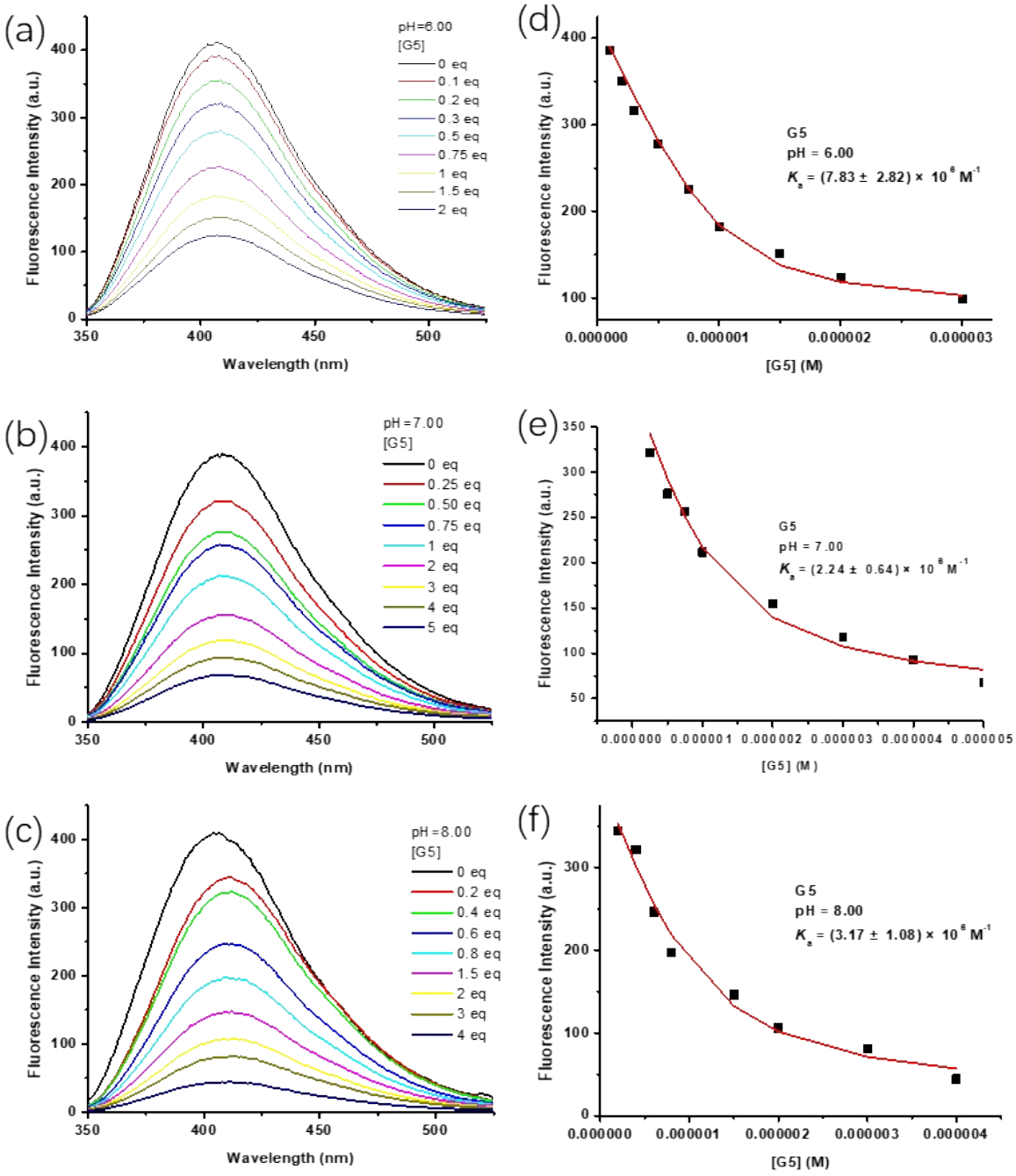

Figure S26. Fluorescence spectra of **WNBP** (1.00 μM) in phosphate buffer solutions (1.0 mM) recorded in the presence of different concentrations of **G5** at 298 K, (a) pH=6.00, (b) pH=7.00, (c) pH=8.00. Nonlinear least-squares analyses used to calculate the K_a value, (d) pH=6.00, (e) pH=7.00, (f) pH=8.00.

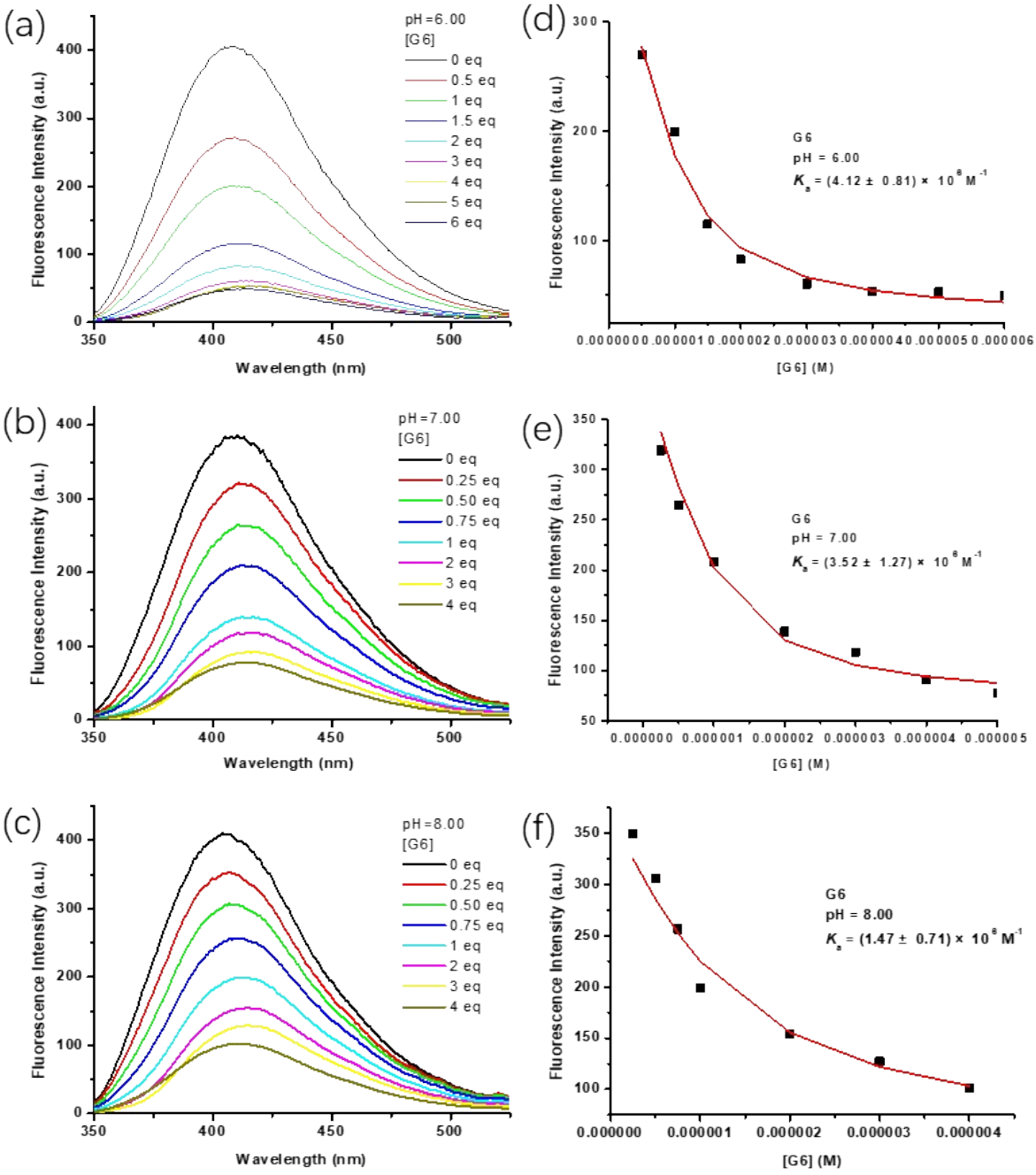

Figure S27. Fluorescence spectra of **WNBP** (1.00 μM) in phosphate buffer solutions (1.0 mM) recorded in the presence of different concentrations of **G6** at 298 K, (a) pH=6.00, (b) pH=7.00, (c) pH=8.00. Nonlinear least-squares analyses used to calculate the K_a value, (d) pH=6.00, (e) pH=7.00, (f) pH=8.00.

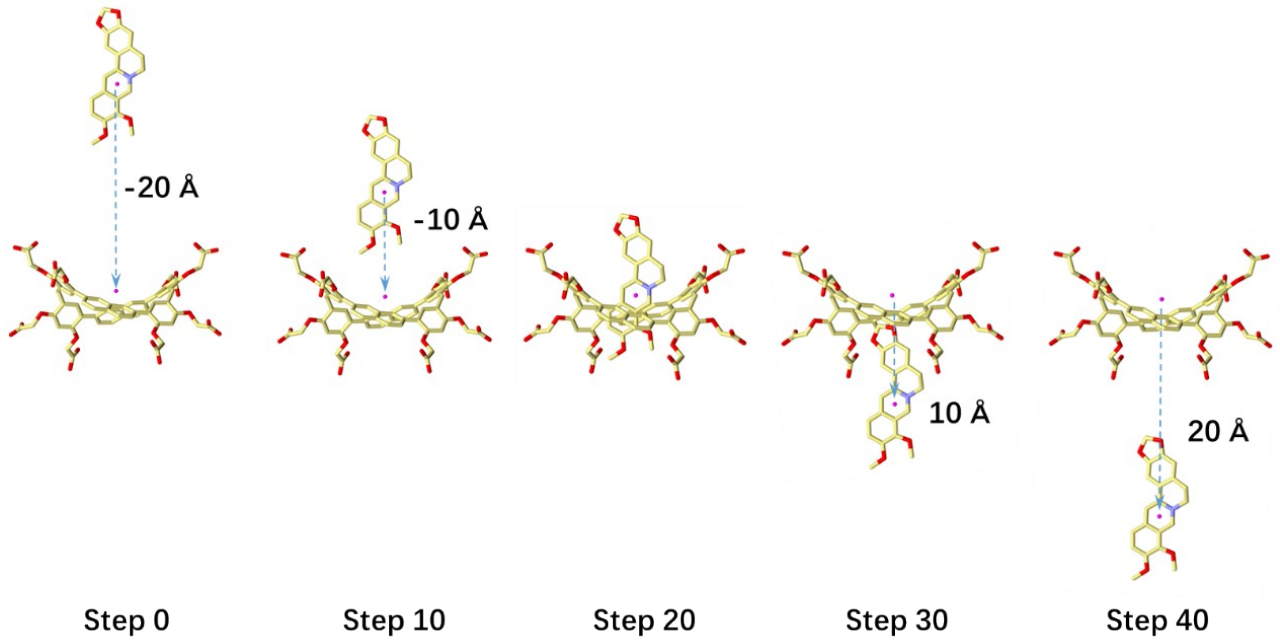

Figure S28. Rigid potential energy surface (PES) scan of the **WNPB-G1** complex, 1.0 Å/step, 40 steps.

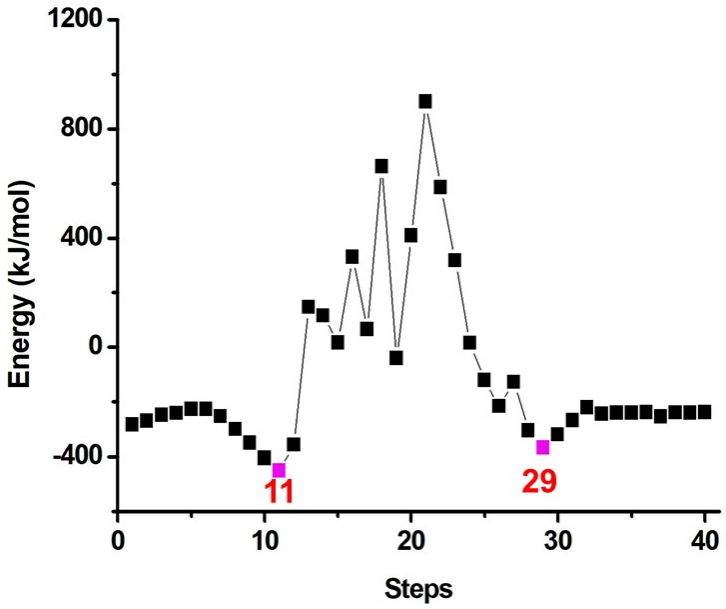

Figure S29. The Change of single point energy in the rigid potential energy surface scan of the **WNPB-G1** complex, 1.0 Å/step, 40 steps.